Copper Carboxylate-phosphonates: Syntheses, Crystal Structures and Magnetic Properties①

XU Yan②

(*Department of Materials Science and Engineering, Suqian University, Suqian* 223800, *China*)

ABSTRACT Two novel copper carboxyly-phosphonates, namely, $Cu_{2.5}$(5-pnc)$(SO_4)_{0.5}(OH)(H_2O)_{0.5}$ (**1**) and $Cu_{0.5}$(5-pncH_2)$(H_2O)_{1.5}$ (**2**) (5-pncH_3 = 5-phosphono-1-naphthalenecarboxylic acid), have been synthesized and characterized by X-ray diffraction, infrared spectroscopy, elemental analysis, and thermogravimetric analysis. In compound **1**, each {PO_3C} tetrahedron is corner-shared with two {Cu(1)O_4}, two {Cu(2)O_5} and one {Cu(3)O_5}, thus forming a one-dimensional inorganic chain along the *c* axis containing 8-membered rings of [Cu_3O_4S] and 19-membered cages of [$Cu_5O_{10}P_4$]. The inorganic chains are further connected by a 5-pnc^{3-} ligand to generate a three-dimensional framework. Compound **2** exhibits a one-dimensional structure, in which the inorganic chains of [Cu-O-Cu]$_n$ are connected by the organic ligands through hydrogen bonding interactions, forming an infinite two-dimensional layer. Magnetic measurements of **1** indicate that dominant antiferromagnetic interactions are mediated between the Cu^{2+} centers.

Keywords: copper, carboxylate-phosphonate, crystal structure, magnetic properties;

DOI: 10.14102/j.cnki.0254–5861.2011–3085

1 INTRODUCTION

Metal phosphonate materials have been receiving an increasing amount of attention due to their significance in the fields of ion-exchange, catalysis, and gas adsorption, as well as having optical, magnetic and proton conducting properties[1-8]. Great efforts have been devoted to the syntheses of metal phosphonates with versatile architectures and interesting physical or chemical functions during the past two decades[9-11]. Among them, metal phosphonates containing carboxylate groups are of particular interest as they provide additional coordination sites for metal ions[12, 13]. A series of metal phosphonate compounds have been reported based on 2/3/4-carboxyphenylphosphonic acid (2/3/4-cppH_3), featuring 1D, 2D and 3D structures, together with interesting magnetic, dielectric and chiroptical properties[14-18]. The (4-carboxynaphthalen-1-yl)phosphonic acid (4-cnappH_3) is analogues to 4-cppH_3 except with an expanded aromatic moiety. Some metal phosphonates based on this ligand have been described, including a cobalt compound with a 3D framework structure showing enantioenrichment[19] and three copper compounds with layered structures[20], as well as four manganese phosphonates with 3D framework or 2D layered structures[21]. However, the 5-phosphono-1-naphthalenecarboxylic acid (5-pncH_3) is a positional isomeric ligand of 4-cnappH_3. As far as we are aware, only one example of metal phosphonates based on this ligand has been reported[22].

To explore new aromatic carboxylate-phosphonate materials, herein we report two new copper phosphonates based on 5-pncH_3, formulated as $Cu_{2.5}$(5-pnc)$(SO_4)_{0.5}(OH)(H_2O)_{0.5}$ (**1**) and $Cu_{0.5}$(5-pncH_2)$(H_2O)_{1.5}$ (**2**). Compound **1** shows a 3D framework structure, whereas **2** exhibits a 1D chain structure. The magnetic properties of compounds **1** and **2** are also investigated.

2 EXPERIMENTAL

2. 1 Materials and physical measurements

All reagents and solvents employed in this work were commercially available and used without further purification. (5-Carboxynaphthalen-1-yl)phosphonic acid (5-pncH_3) was

Received 4 January 2021; accepted 12 May 2021 (**CCDC 2053627** for **1** and **2036514** for **2**)

① Supported financially by Suqian Sci & Tech Program (No. K201911) and the second batch of university-level scientific research platform of Suqian University (No. 2021pt04)

② Corresponding author. E-mail: xuyan0511@126.com

synthesized following a previous procedure[19]. Elemental analyses (C and H) were performed on a Perkin-Elmer 240C elemental analyzer. IR spectra were recorded on a Bruker Tensor 27 spectrometer in the range of 400～4000 cm^{-1} using KBr pellets. Thermal analyses were performed using a Mettler Toledo TGA/DSC thermoanalyzer in a temperature range of 50～800 °C in N_2 flow (20 mL/min) at a heating rate of 10 °C/min. Powder X-ray diffraction (XRD) data were collected on a Bruker D8 ADVANCE X-ray powder diffractometer with Cu$K\alpha$ radiation (λ = 1.54056 Å) in a range of 5.00～50.00° at room temperature. The magnetization data were recorded on a Quantum Design MPMS-XL7 SQUID magnetometer and a vibrating sample magnetometer (VSM) of the Quantum Design MPMS SQUID VSM system. The diamagnetic contribution of the sample itself was estimated from Pascal's constant[23].

2. 2 Synthesis of $Cu_{2.5}$(5-pnc)$(SO_4)_{0.5}(OH)(H_2O)_{0.5}$ (1)

A mixture of $Cu(SO_4)_2$ $5H_2O$ (0.2 mmol, 0.0512 g), 5-pncH_3 (0.1mmol, 0.0256 g) and 10 mL of a mixed solution of H_2O/methanol (1:1 in volume) was kept in a Teflon-lined autoclave at 140 °C for 2 days. After cooling the autoclave to room temperature, light green block-like crystals were obtained as a monophasic material, judged by powder X-ray diffraction pattern. Yield: 43.9% based on 5-pncH_3. Elemental analysis (%) calcd. for $C_{11}H_9O_9PS_{0.5}Cu_{2.5}$: C, 26.90; H, 1.85. Found: C, 26.53; H, 1.76. IR (KBr, cm^{-1}): 3554m, 3125br, 1596w, 1541s, 1402m, 1381m, 1327w, 1205w, 1089s, 1041s, 956s, 801m, 771m, 591m, 543w, 498w, 466w.

2. 3 Synthesis of $Cu_{0.5}$(5-pncH_2)$(H_2O)_{1.5}$ (2)

The $Cu(ClO_4)_2$ $6H_2O$ (0.2 mmol, 0.0742 g), 5-pncH_3 (0.1mmol, 0.0254 g) and 10 mL water were stirred for 2 h. Then two drops of 0.5 M NaOH were added into the solution. The mixture was kept in a Teflon-lined autoclave at 140 ℃ for 2 days. After cooling the autoclave to room temperature, light green rod-like crystals were obtained as a monophasic material, judged by powder X-ray diffraction pattern. Yield: 10.3% based on 5-pncH_3. Elemental analysis (%) calcd. for $C_{11}H_{11}O_{6.5}PCu_{0.5}$: C, 42.62; H, 3.55. Found: C, 42.31; H, 3.51. IR (KBr, cm^{-1}): 2985br, 2645m, 1681s, 1511m, 1427m, 1334w, 1295m, 1132s, 1065s, 1028s, 917m, 802s, 594m, 534w, 502w, 464w.

2. 4 X-ray data collection and structure determination

Single crystals of **1** (0.12mm × 0.12mm × 0.11mm) and **2** (0.20mm × 0.20mm × 0.20mm) were used for indexing and intensity data collection on a Bruker APEX II CCD diffractometer using graphite-monochromated Mo$K\alpha$ radiation (λ = 0.71073 Å) at 293 K. A hemisphere of data was collected in the θ ranges of 4.2730～70.9370 ° for **1** and 2.1070～73.5890 ° for **2**. The data were integrated using the Siemens SAINT program[24], with the intensities corrected for Lorentz factor, polarization, air absorption, and absorption due to variation in the path length through the detector faceplate. Empirical absorption and extinction corrections were applied. The structures were solved by direct methods and refined on F^2 by full-matrix least-squares using SHELXL[25]. All the non-hydrogen atoms were located from Fourier maps, and refined anisotropically. All H atoms were put in calculated positions using the riding mode, and refined isotropically with the isotropic vibration parameters related to the non-H atom to which they are bonded. Crystallographic data and selected bond lengths and bond angles for compounds **1** and **2** are listed in Tables 1 and 2, respectively.

Table 1. Crystallographic Data for Compounds 1 and 2

Compound	**1**	**2**
Formula	$C_{11}H_9O_9PS_{0.5}Cu_{2.5}$	$C_{11}H_{11}O_{6.5}PCu_{0.5}$
M_r	491.03	309.95
Crystal system	Monoclinic	Orthorhombic
Space group	*C*2/*c*	*Pbcm*
a (Å)	27.0081(16)	6.6788(2)
b (Å)	11.5406(5)	8.8414(2)
c (Å)	10.0047(7)	41.7403(9)
V (Å^3)	2666.2(4)	2464.76(11)
D_c (g cm^{-3})	2.447	1.670
μ (mm^{-1})	7.133	3.112
F(000)	1940	1268
R_{int}	0.0323	0.0307

To be continued

GOOF on F^2	1.057	1.049
R, wR^a ($I > 2\sigma(I)$)	0.0621, 0.1572	0.0360, 0.0986
R, wR^a (all data)	0.0742, 0.1672	0.0408, 0.1030
$(\Delta\rho)_{max}$, $(\Delta\rho)_{min}$/e·Å^{-3}	0.929, –1.479	0.358, –0.372

$^aR = \Sigma||F_o| - |F_c||/\Sigma|F_o|$, $wR = [\Sigma w(F_o^2 - F_c^2)^2/\Sigma w(F_o^2)^2]^{1/2}$

Table 2. Selected Bond Lengths (Å) and Bond Angles (°)

1					
Bond	Dist	Bond	Dist	Bond	Dist
Cu(1)–O(3A)	1.910(5)	Cu(2)–O(6)	2.156(11)	Cu(3)–O(6)	1.991(9)
Cu(1)–O(1)	2.025(5)	Cu(2)–O(5)	2.197(10)	Cu(3)–O(6D)	1.993(10)
Cu(2)–O(1)	1.990(6)	Cu(3)–O(7)	1.968(11)	Cu(3)–O(8)	1.900(8)
Cu(2)–O(2A)	2.001(4)	Cu(3)–O(2A)	1.978(7)		
Angle	(°)	Angle	(°)	Angle	(°)
O(3A)–Cu(1)–O(3B)	166.0(3)	O(4E)–Cu(2)–O(6)	90.4(3)	O(7)–Cu(3)–O(2A)	126.0(5)
O(3A)–Cu(1)–O(1)	90.13(18)	O(1)–Cu(2)–O(6)	171.6(3)	O(8F)–Cu(3)–O(6)	158.3(5)
O(3B)–Cu(1)–O(1)	89.95(19)	O(2A)–Cu(2)–O(6)	81.4(3)	O(7)–Cu(3)–O(6)	98.5(5)
O(3A)–Cu(1)–O(1C)	89.95(19)	O(4E)–Cu(2)–O(5)	90.3(3)	O(2A)–Cu(3)–O(6)	86.2(4)
O(3B)–Cu(1)–O(1C)	90.13(18)	O(1)–Cu(2)–O(5)	103.8(3	O(8F)–Cu(3)–O(6D)	93.4(4)
O(1)–Cu(1)–O(1C)	179.3(3)	O(2A)–Cu(2)–O(5)	108.5(3)	O(7)–Cu(3)–O(6D)	110.0(6)
O(4E)–Cu(2)–O(1)	93.4(2)	O(6)–Cu(2)–O(5)	83.7(4)	O(2A)–Cu(3)–O(6D)	120.2(3)
O(4E)–Cu(2)–O(2A)	158.3(2)	O(8F)–Cu(3)–O(7)	89.7(4)	O(6)–Cu(3)–O(6D)	64.9(6)
O(1)–Cu(2)–O(2A)	92.4(2)	O(8F)–Cu(3)–O(2A)	105.3(3)		
2					
Bond	Dist	Bond	Dist	Bond	Dist
Cu(1)–O(1A)	1.9802(16)	Cu(1)–O(4A)	2.0010(17)	Cu(1)–O(5)	2.245(3)
Cu(1)–O(1)	1.9802(16)	Cu(1)–O(4)	2.0012(17)	Cu(1)–O(5B)	2.675(4)
Angle	(°)	Angle	(°)	Angle	(°)
O(1A)–Cu(1)–O(1)	89.22(9)	O(1A)–Cu(1)–O(5)	89.89(7)	O(1A)–Cu(1)–O(5B)	99.27(1)
O(1A)–Cu(1)–O(4)	90.03(7)	O(1)–Cu(1)–O(5)	89.89(7)	O(1)–Cu(1)–O(5B)	99.27(1)
O(1)–Cu(1)–O(4)	175.16(7)	O(4A)–Cu(1)–O(4)	90.32(11)	O(5A)–Cu(1)–O(5)	167.09(1)
O(1A)–Cu(1)–O(4A)	175.16(7)	O(4A)–Cu(1)–O(5)	94.89(7)	O(4A)–Cu(1)–O(5B)	76.13(9)
O(1)–Cu(1)–O(4A)	90.03(7)	O(4)–Cu(1)–O(5)	94.89(7)	O(4)–Cu(1)–O(5B)	76.13(9)

Symmetry codes: A –*x*+2, –*y*+2, –*z*+2; B *x*, –*y*+2, *z*–1/2; C –*x*+2, *y*, –*z*+3/2; D –*x*+2, *y*, –*z*+5/2; E –*x*+3/2, *y*–1/2, –*z*+3/2; F *x*+1/2, *y*–1/2, *z*+1 for **1**; A: *x*, *y*, 0.5–*z*; B: 1–*x*, –0.5+*y*, 0.5–*z* for **2**

3 RESULTS AND DISCUSSION

3. 1 Crystal structures of 1 and 2

Compounds **1** and **2** were synthesized by reactions of ligand 5-pncH$_3$ and different copper salts ($Cu(SO_4)_2$·5H$_2$O for **1** and $Cu(ClO_4)_2$·6H$_2$O for **2**) at 140 ℃ under solvothermal for **1** and hydrothermal for **2** reaction conditions (Fig. 1a). Although the carboxyly-phosphonate acid ligand and metal are the same, their structures are completely different. It is found that the anions of metal original play critical roles in self-assembly.

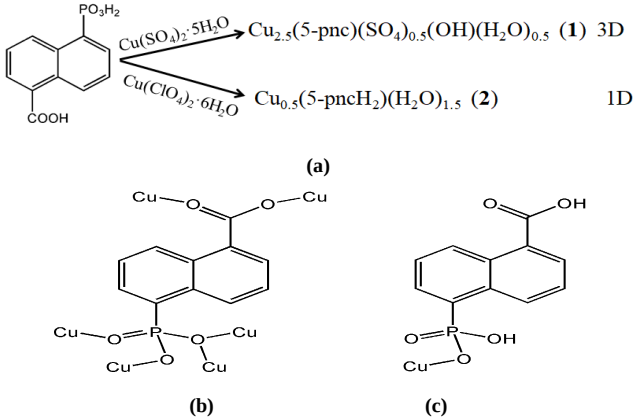

Fig. 1. (a) Schematic synthesis of 1 and 2. Coordination modes of 5-pncH$_3$ in compounds 1 (b) and 2 (c)

Single crystal structural determination reveals that **1** crystalizes in monoclinic system, space group *C*2/*c*. Each asymmetric unit of compound **1** consists of 2.5 Cu atoms, 1 5-pnc^{3-} ligand, 0.5 coordination SO_4^{2-}, 1 coordination OH^-, and 0.5 coordination H_2O. The Cu(1) displays a distorted planar quadrilateral geometry. Four coordination sites are occupied by four phosphonate oxygen atoms (O(1), O(1A), O(3B), O(3C)) from four equivalent 5-pnc^{3-} ligands (Symmetry codes: A: 2–*x*, *y*, 1.5–*z*; B: 2–*x*, 2–*y*, 2–*z*; C: *x*, 2–*y*, –0.5+*z*). Cu(2) and Cu(3) are each five-coordinated with a distorted trigonal-bipyramidal geometry, surrounded by two phosphonate oxygen, one carboxylate oxygen, one hydroxyl oxygen, and one sulfate oxygen atoms for Cu(2) and one phosphonate oxygen, one carboxylate oxygen, two hydroxyl oxygen, and water molecule oxygen atoms for Cu(3) (Fig. 2a). The Cu–O bond lengths (1.900(8) ~ 2.197(10) Å) are comparable to those in the other copper phosphonate compounds[20].

The 5-pnc^{3-} ligand is fully deprotonated. It serves as a hepta-dentate ligand connecting seven Cu atoms using its three phosphonate oxygen and two carboxylate oxygen donors (Fig. 1b). Each SO_4^{2-} behaves as a bidentate metal linker bridging two equivalent Cu atoms through two oxygen atoms. Each OH^- acts μ_3-O(H) bridging three Cu atoms. Each {PO_3C} tetrahedron is corner-shared with two {Cu(1)O_4}, two {Cu(2)O_5} and one {Cu(3)O_5}, thus forming a one-dimensional inorganic chain along the *c* axis containing 8-membered rings of [Cu_3O_4S] and 19-membered cages of [$Cu_5O_{10}P_4$] (Fig. 2b). The inorganic chains are further connected by a 5-pnc^{3-} ligand, generating a three-dimensional framework (Fig. 2c).

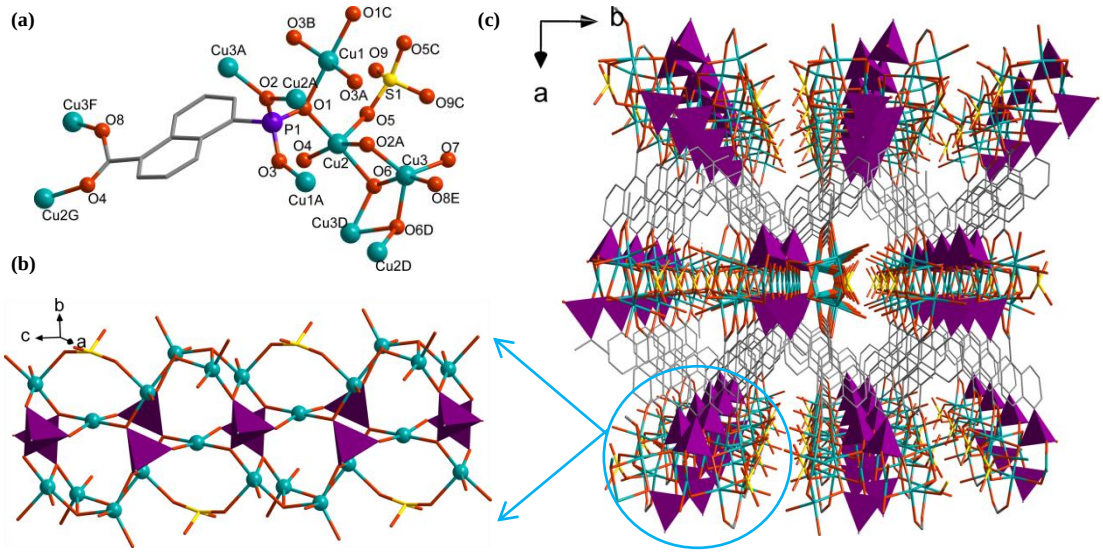

Fig. 2. (a) Building unit with labelling except carbon atoms in compound 1. (b) The inorganic chain of structure. (c) Packing diagram of structure 1 viewed along the *c* axis. The hydrogen atoms attached to carbon are omitted for clarity. Symmetry codes: A: –*x*+2, –*y*+2, –*z*+2; B: *x*, –*y*+2, *z*–1/2; C: –*x*+2, *y*, –*z*+3/2; D: –*x*+2, *y*, –*z*+5/2; E: *x*+1/2, *y*–1/2, *z*+1; F: *x*–1/2, *y*+1/2, *z*–1; G –*x*+3/2, *y*+1/2, *z*+3/2

Compound **2** crystallizes in orthorhombic space group *Pbcm*. The asymmetric unit contains 0.5 Cu^{2+} ion, 1 5-pncH_2^- and 1.5 coordination water molecules (Fig. 3b). The Cu^{2+} ion has a distorted square-pyramidal coordination environment. The basal positions are occupied by two phosphonate oxygens from two equivalent 5-pncH_2^- ligands, and two water molecule oxygen atoms (Cu–O: 1.9802(16)~ 2.0012(17) Å). The apical position is filled with coordination water molecule oxygen atoms, presenting an elongated Cu–O(5A) bond length (2.245(3) Å), which is similar to those reported in other Cu^{2+} phosphonates[20]. In addition, O(5B) from another coordination water molecule shows a weak contact with the Cu^{2+} ion (Cu(1)–O(5B): 2.675(4) Å), thus forming an inorganic chain running along the b axis containing [Cu–O–Cu]$_n$.

The 5-pncH_2^- ligand is singly protonated at O3 and O7. It serves as a monodentate ligand, coordinating one Cu^{2+} ion through its one phosphonate oxygen atom (Fig. 1c). The naphthalenecarboxyly groups of 5-pncH_2^- ligand are pendant on the two sides of the inorganic chain (Fig. 3a). C–H···π

stacking interaction (3.412 Å) is observed among the adjacent naphthalene rings of the 5-pncH$_2^-$ ligand. The inorganic chains are further connected by organic ligands through hydrogen bond interactions (O(6)···O(7) = 2.7031 Å) from neighbouring carboxyly groups. Consequently, an infinite 2-D layer in the *bc* plane is constructed (Fig. 3b).

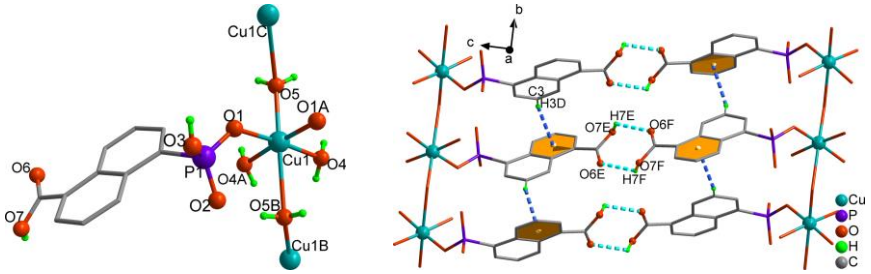

(a) **(b)**

Fig. 3. (a) Building unit with labelling except carbon atoms in compound 2. (b) Hydrogen bond interactions and C–H···π stacking interaction for structure 2. All H atoms except those attached to the COO$^-$ are omitted for clarity. Symmetry codes: A: *x*, *y*, –*z*+1/2; B: –*x*+1, *y*–1/2, –*z*+1/2; C: –*x*+1, *y*+1/2, –*z*+1/2; D: *x*+1, –*y*+1/2, –*z*+1; E: –*x*+2, –*y*+1, –*z*+1; F: *x*+1, *y*, *z*

3. 3 FTIR and powder X-ray diffraction

The FTIR spectra of ligand 5-pncH$_3$, compounds **1** and **2** are shown in Fig. 4a. The bands appearing at 1695, 1266 cm^{-1} and 1687, 1289 cm^{-1} (for 5-pncH$_3$ and compound **2**) correspond to the stretching vibration of uncoordinated COO, while the peaks of coordinated COO appear at 1542, 1412 cm^{-1}. The enhanced intensity at 1136 and 620 cm^{-1} is attributed to the ClO$_4^-$ anion in compound **1**. The vibration bands of phosphonate groups appear at 1098, 1058, 1020 and 948 cm^{-1} for ligand 5-pncH$_3$, 1094, 1044 and 948 cm^{-1} for compound **1** and 1126, 1067, 1027 and 916 cm^{-1} for compound **2**. The results indicate that the coordination modes of carboxylate and phosphonate groups are different in compounds **1** and **2**. The experimental and simulated powder X-ray diffraction (PXRD) patterns of **1** and **2** are shown in Fig. 4b and 4c. The experimental PXRD patterns at room temperature are in good agreement with the simulated ones based on single-crystal X-ray solution, demonstrating the phase purity of the bulk products. The differences in reflection intensities are probably due to the preferred orientation effects.

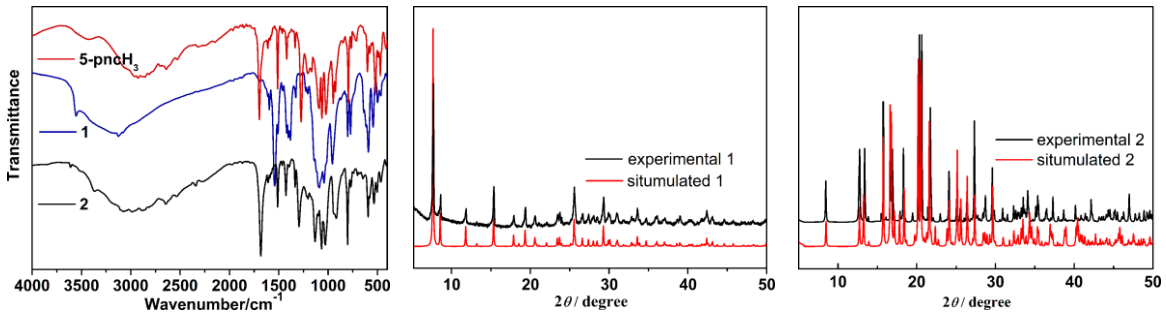

(a) **(b)** **(c)**

Fig. 4. FTIR spectra (a) and PXRD patterns for compounds 1 (b) and 2 (c)

3. 4 Thermal stability

To compare their thermal stabilities, thermogravimetric analyses were performed on fresh samples under a nitrogen gas flow. Compound **1** shows a three-step decomposition process, indicating its stability below 290 ℃. The organic components decompose and the structure collapses above 290 ℃. Compound **2** also experiences a three-step decomposition in the temperature range of 50～800 ℃, as shown in Fig. 5. The first step is observed below 140 ℃ with weight loss of 4.5%, and the second step in the 260～350 ℃ region to 4.3%. The total weight loss is 8.8%, which corresponds to the removal of 1.5 water molecules (calcd. 8.72%). The third steps observed above 350 ℃ are attributed to the burning of organic components and the collapse of the framework structure.

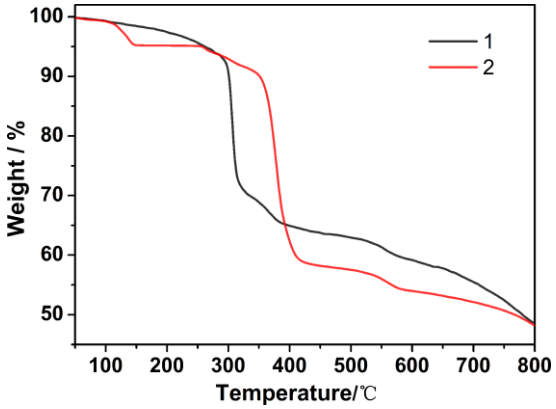

Fig. 5. Thermogravimetric analyses for compounds 1 and 2

3. 5 Magnetic properties

The magnetic properties of the two compounds were investigated using polycrystalline samples. Fig. 6 shows $\chi_M T$ vs. T plots of compounds **1** and **2** measured under a dc field of 1000 Oe. The room temperature $\chi_M T$ value per Cu is 0.41 and 0.43 cm^3 K mol^{-1} for compounds **1** and **2**, respectively, close to that expected for non-interacting Cu^{2+} ions with S = 1/2 and g = 2.2 (0.45 cm^3 K mol^{-1}). The $\chi_M T$ value decreases continuously upon cooling, suggesting that antiferromagnetic (AF) interaction is dominant between the magnetic centers. The presence of AF interaction is also confirmed by a larger negative Weiss constant (–148.5, –59.46 K for compounds **1** and **2**, respectively), determined by the susceptibility data above 100 K.

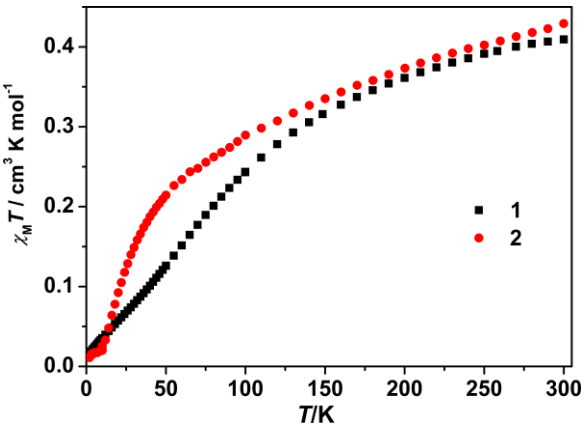

Fig. 6. Temperature dependence of $\chi_M T$ (□) and $1/\chi_M$ (○) for compound 1

4 CONCLUSION

In conclusion, the syntheses, structures and magnetic properties of two new copper carboxylate phosphonates based on 5-pncH$_3$ ligand, namely, $Cu_{2.5}$(5-pnc)$(SO_4)_{0.5}(OH)(H_2O)_{0.5}$ (**1**) and $Cu_{0.5}$(5-pncH$_2$)$(H_2O)_{1.5}$ (**2**), have been reported. Compound **1** features a three-dimensional framework structure with inorganic chains connected by the 5-pncH$^-$ ligand, while compound **2** displays a one-dimensional structure in which the inorganic chains are connected by organic ligands through hydrogen bond interactions, forming an infinite 2-D layer. Magnetic measurements reveal that dominant antiferromagnetic interactions are mediated between the Cu^{2+} centers in compounds **1** and **2**.

REFERENCES

(1) Cleareld, A.; Demadis, K. Metal phosphonate chemistry: from synthesis to applications. *RSC* **2012**.

(2) Yucesan, G.; Zorlu, Y.; Stricker, M.; Beckmann, J. Metal-organic solids derived from arylphosphonic acids. *Coord. Chem. Rev.* **2018**, 369, 105–122.

(3) Gelfand, B. S.; Huynh, R. P. S.; Mah, R. K.; Shimizu, G. K. H. Mediating order and modulating porosity by controlled hydrolysis in a phosphonate monoester metal-organic framework. *Angew. Chem., Int. Ed*. **2016**, 55, 14614–14617.

(4) Adelani, P. O.; Albrecht-Schmitt, T. E. Comparison of thorium(IV) and uranium(VI) carboxyphosphonates. *Inorg. Chem*. **2010**, 49, 5701–5705.

(5) Zeng, T.; Wang, L.; Feng, L.; Xu, H.; Cheng, Q.; Pan, Z. Two novel organic phosphorous-based MOFs: synthesis, characterization and photocatalytic properties. *Dalton Trans*. **2019**, 48, 523–534.

(6) Liu, Q. Y.; Xiong, W. L.; Liu, C. M.; Wang, Y. L.; Wei, J. J.; Xiahou, Z. J.; Xiong, L. H. Chiral induction in the ionothermal synthesis of a 3D chiral heterometallic metal-organic framework constructed from achiral 1,4-naphthalenedicarboxylate. *Inorg. Chem.* **2013**, 52, 12, 6773–6775.

(7) Li, R. P.; Liu, Q. Y.; Wang, Y. L.; Liu, C. M.; Liu, S. J. Evolution from linear tetranuclear clusters into one-dimensional chains of Dy(III) single-molecule magnets with an enhanced energy barrier. *Inorg. Chem. Front.* **2017**, 4, 1149–1156.

(8) Wang, Y. L.; Han, C. B.; Zhang, Y. Q.; Liu, Q. Y.; Liu, C. M.; Yin, S. G. Fine-tuning ligand to modulate the magnetic anisotropy in a carboxylate-bridged Dy2 single-molecule magnet system. *Inorg. Chem.* **2016**, 55, 5578–5584.

(9) Bhanja, P.; Na, J.; Jing, T.; Lin, J. J.; Wakihara, T.; Bhaumik, A.; Yamauchi, Y. Nanoarchitectured metal phosphates and phosphonates: a new material horizon toward emerging applications. *Chem. Mater*. **2019**, 31, 5343–5362.

(10) Xu, Y.; Li, X. X.; Wang, H. X.; Liu, H. R. Synthesis, crystal structure and luminescence of one-dimensional homochiral terbium(III) coordination polymers. *Chin. J. Struct. Chem*. **2020**, 6, 1044–1050.

(11) Weng, G. G.; Zheng, L. M. Chiral metal phosphonates: assembly, structures and functions. *Sci. China Chem*. **2020**, 63, 619–636.

(12) Liu, B.; Liu, J. C.; Shen, Y.; Feng, J. S.; Bao, S. S.; Zheng, L. M. Polymorphic layered copper phosphonates: exfoliation and proton conductivity studies. *Dalton Trans*. **2019**, 48, 6539–6545.

(13) Feng, J. S.; Bao, S. S.; Ren, M.; Cai, Z. S.; Zheng, L. M. Chirality- and pH-controlled supramolecular isomerism in cobalt phosphonates and its impact on the magnetic behavior. *Chem. Eur. J.* **2015**, 21, 17336–17343.

(14) Zima, V.; Svoboda, J.; Benes, L. Synthesis and characterization of copper 4-carboxyphenylphosphonates. *J. Solid State Chem.* **2009**, 182, 3155–3161.

(15) Zang, D. M.; Cao, D. K.; Zheng, L. M. Strontium and barium 4-carboxylphenylphosphonates: hybrid anti-corrosion coatings for magnesium alloy. *Inorg. Chem. Commun*. **2011**, 14, 1920–1923.

(16) Putz, A. M.; Carrella, L. M.; Rentschler, E. A distorted honeycomb motif in divalent transition metal compounds based on 4-phosphonbenzoic acid and exchange coupled Co(II) and Cu(II): synthesis, structural description and magnetic properties. *Dalton Trans*. **2013**, 42, 16194–16199.

(17) Li, J. T.; Cao, D. K; Akutagawa, T.; Zheng, L. M. $Zn_3(4\text{-}OOCC_6H_4PO_3)_2$: a polar metal phosphonate with pillared layered structure showing SHG-activity and large dielectric anisotropy. *Dalton Trans*. **2010**, 39, 8606–8608.

(18) Wang, P. F.; Bao, S. S.; Huang, X. D.; Akutagawa, T.; Zheng, L. M. Temperature controlled formation of polar copper phosphonates showing large dielectric anisotropy and a dehydration-induced switch from ferromagnetic to antiferromagnetic interactions. *Chem. Commun.* **2018**, 54, 6276–6279.

(19) Liu, B.; Xu, Y.; Bao, S. S.; Huang, X. D.; Liu, M.; Zheng, L. M. Enantioenriched cobalt phosphonate containing Δ–type chains and showing slow magnetization relaxation. *Inorg. Chem.* **2016**, 55, 9521–9523.

(20) Liu, B.; Liu, J. C.; Shen, Y.; Feng, J. S.; Bao, S. S.; Zheng, L. M. Polymorphic layered copper phosphonates: exfoliation and proton conductivity studies. *Dalton Trans.* **2019**, 48, 6539–6545.

(21) Liu, B.; Bao, S. S.; Ren, M.; Cai, Z. S.; Liu, J. C.; Zheng, L. M. Syntheses, structures and magnetic properties of manganese phosphonates. *Chin. J. Inorg. Chem.* **2020**, 36, 1185–1194.

(22) Xu, Y.; Liu, B.; Li, J.; Gao, L. A manganese(II) coordination polymer constructed from phosphonate ligand: synthesis, crystal structure and magnetic properties. *Chin. J. Struct. Chem*. **2021**, DOI:10.14102/j.cnki.0254–5861.2011–2852.

(23) Kahn, O. *Molecular Magnetism.* VCH Publishers, Inc., New York **1993**.

(24) *SAINT, Program for Data Extraction and Reduction*. Siemens Analytical X-ray Instruments, Madison, WI **1994–1996**.

(25) *SHELXTL* (*Version 5.0*), *Reference Manual. Siemens Industrial Automation*. Analytical Instruments: Madison, WI **1995**.